

Experimental Mg ix photorecombination rate coefficient

S. Schippers¹, M. Schnell², C. Brandau¹, S. Kieslich¹, A. Müller¹, and A. Wolf²

¹ Institut für Kernphysik, Justus-Liebig-Universität Giessen, Leihgesterner Weg 217, D-35392 Giessen, Germany
e-mail: Stefan.E.Schippers@strz.uni-giessen.de

² Max-Planck-Institut für Kernphysik, Saupfercheckweg 1, D-69117 Heidelberg, Germany

Received / Accepted

Abstract. The rate coefficient for radiative and dielectronic recombination of berylliumlike magnesium ions was measured with high resolution at the Heidelberg heavy-ion storage ring TSR. In the electron-ion collision energy range 0–207 eV resonances due to $2s \rightarrow 2p$ ($\Delta N = 0$) and $2s \rightarrow 3l$ ($\Delta N = 1$) core excitations were detected. At low energies below 0.15 eV the recombination rate coefficient is dominated by strong $1s^2(2s2p^3P)7l$ resonances with the strongest one occurring at an energy of only 21 meV. These resonances decisively influence the Mg ix recombination rate coefficient in a low temperature plasma. The experimentally derived Mg ix dielectronic recombination rate coefficient ($\pm 15\%$ systematical uncertainty) is compared with the recommendation by Mazzotta et al. (1998, A&AS, 133, 403) and the recent calculations by Gu (2003, ApJ, 590, 1131) and by Colgan et al. (2003, A&A, 412, 597). These results deviate from the experimental rate coefficient by 130%, 82% and 25%, respectively, at the temperature where the fractional abundance of Mg ix is expected to peak in a photoionized plasma. At this temperature a theoretical uncertainty in the $1s^2(2s2p^3P)7l$ resonance positions of only 100 meV would translate into an uncertainty of the plasma rate coefficient of almost a factor 3. This finding emphasizes that an accurate theoretical calculation of the Mg ix recombination rate coefficient from first principles is challenging.

Key words. atomic data – atomic processes – line: formation – plasmas – radiation mechanisms: general

1. Introduction

For the accurate calculation of the ionization equilibrium in astrophysical plasmas, rate coefficients for the population and depopulation of the various ion charge states have to be known precisely. To date most of the required rate coefficients are derived from theoretical calculations, and, hence, experimental benchmarks are required for testing and improving the theoretical methods. This is especially true for recombination in photoionized plasmas, which occurs at relatively low plasma temperatures of only a few electron volts. At such low temperatures the recombination rate coefficient, depending on the ion under consideration, can strongly be influenced by the existence of low-energy dielectronic recombination (DR) resonances that are difficult to theoretically predict with sufficient accuracy.

Experimentally derived plasma rate coefficients were previously published for the recombination of C iv (Schippers et al. 2001), O vi (Böhm et al. 2003), Ti v (Schippers et al. 1998), Ni xviii (Fogle et al. 2003), Ni xxvi (Schippers et al. 2000) and Fe xviii – Fe xxii (Savin et al. 1997, 1999, 2002a,b, 2003). Here the Mg ix recombination rate coefficient derived from experimental measurements at a heavy ion storage ring is provided.

The approximate temperature ranges where berylliumlike magnesium forms in photoionized and in collisionally ionized plasmas can be obtained from the work of Kallman & Bautista (2001) who calculated the fractional abundances of ions in plasmas for a variety of physical conditions. For photoionized plasmas they find that the fractional Mg ix abundance peaks at an ionization parameter of $\log \zeta = 0.9$ corresponding to a temperature of about 2.8 eV. The ‘photoionized zone’ may be defined as the range of temperatures where the fractional abundance of a given ion exceeds 10% of its peak value. For Mg ix this corresponds to the temperature range 2–13 eV. Using the same criterion and the results of Kallman & Bautista (2001) for coronal equilibrium the Mg ix ‘collisionally ionized zone’ is estimated to extend over the temperature range 60–170 eV. It should be kept in mind that these temperature ranges are only indicative. In particular, they depend on the accuracy of the atomic data base used by Kallman & Bautista (2001) and, in case of the photoionization zone, on the assumed $1/E$ energy dependence of the ionizing radiation. Nevertheless, the above given temperature ranges will be used in the discussion below.

From the present measurements it is found that the Mg ix recombination rate coefficient in the photoionization zone is decisively influenced by the presence of a strong DR resonance at an electron-ion collision energy of 21 meV. Any theoretical calculation aiming at an accurate Mg ix rate coefficient will

have to predict this resonance's position with an error of less than a few meV. Presently available atomic-structure computer codes are generally not capable of providing results with such an accuracy ab initio. In the standard theoretical approaches the situation is often improved by using spectroscopically observed target energies for the atomic structure (Colgan et al. 2003; Gu 2003a). As will be shown below, a 100 meV uncertainty on the theoretical resonance position would translate into an uncertainty of the Mg ix DR rate coefficient of a factor 2.7 at the temperature where the Mg ix abundance is expected to peak in photoionization equilibrium.

2. Experiment

Various aspects of recombination measurements at the heavy-ion storage ring TSR of the Max-Planck-Institut für Kernphysik (MPI-K) in Heidelberg, Germany, have been described by Kilgus et al. (1992), Lampert et al. (1996), Pastuszka et al. (1996), Müller & Wolf (1997), and Schippers et al. (2000, 2001). For the present experiment a Mg ix ion beam with an energy of about 4.2 MeV/u was provided by the MPI-K linear accelerator facility and injected into the storage ring. There, over a distance of ~ 1.5 m, the ion beam was merged with a collinearly moving, magnetically guided electron beam. The electron beam served two purposes. First, it acted as a coolant for the ion beam, i.e., the ion beam's diameter and momentum spread were reduced by collisions with the much "colder" electrons (electron cooling, Poth 1990). Second, the electron cooling device (electron cooler) was subsequently used as an electron target where the ions recombined with the electrons and thereby changed their charge state. After adjusting the electron energy to a well defined value by tuning the electron cooler's cathode voltage appropriately, recombined ions were separated from the circulating parent-ion beam in the first bending magnet downstream from the electron cooler. Because of their high velocity they were efficiently counted with a scintillation detector. *Absolute* recombination rate coefficients as a function of relative energy between electrons and ions were derived from the measured count rate by i) subtracting the separately measured "background" count rate due to electron capture from residual gas molecules and by ii) normalizing to the number of stored ions and to the electron current which were both continuously monitored during the measurement. The "merged-beams technique" was recently reviewed by Phaneuf et al. (1999).

For the derivation of *absolute* rate coefficients from merged electron-ion beams measurements the contamination of the ion beam by metastable ions is an issue of concern. In a storage-ring experiment metastable ions can usually be given enough time (up to a few seconds) to decay before data taking is started. However, berylliumlike ions with zero nuclear spin like $^{24}\text{Mg ix}$ possess an extremely long-lived metastable $1s^2 2s 2p^3 P_0$ state which cannot decay to the $1s^2 2s^2 1S_0$ ground state by a one-photon transition. DR resonances due to the excitation of the 3P_0 metastable state were observed in *single-pass* merged-beams experiments with berylliumlike ions by Badnell et al. (1991). Such resonances are not observed in the present ex-

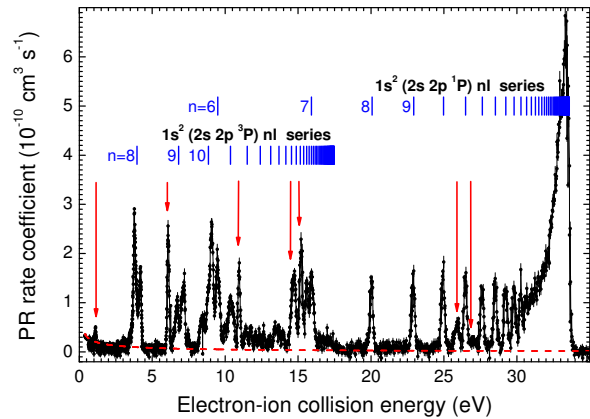


Fig. 1. Measured Mg ix merged-beams recombination rate-coefficient in the electron-ion collision energy region of DR $1s^2 2s 2p nl$ resonances attached to $1s^2 2s^2 \rightarrow 1s^2 2s 2p$ ($\Delta N = 0$) core excitations. The dashed line is the calculated hydrogenic rate coefficient for radiative recombination (RR). Positions of some $1s^2 2p^2 nl$ TR resonances are marked by vertical arrows (see text).

periment. All measured resonances can be attributed to the excitation of Mg ix ground-state ions.

3. Results

The experimental Mg ix merged-beams recombination rate coefficient is shown in Figures 1 – 3 over different ranges of electron-ion collision energy. Figure 1 displays all measured recombination resonances due to $1s^2 2s^2 \rightarrow 1s^2 2s 2p$ and $1s^2 2s^2 \rightarrow 1s^2 2p^2$ ($\Delta N = 0$) core excitations with the exception of the resonances at very low energies below 0.15 eV. These were measured separately with higher resolution and are displayed in Figure 2. Finally, Figure 3 shows at higher energies the DR spectrum for resonances attached to $1s^2 2s^2 \rightarrow 1s^2 2s 3l$ ($\Delta N = 1$) core excitations.

3.1. $\Delta N = 0$ di- and trielectronic recombination

Most of the measured $\Delta N = 0$ photorecombination resonances in Figure 1 can be ascribed to $1s^2 2s^2 \rightarrow 1s^2 (2s 2p^3 P)$ and $1s^2 2s^2 \rightarrow 1s^2 (2s 2p^1 P)$ excitations. The corresponding Rydberg series of DR resonances converge to their respective series limits. Their spectroscopic values are 17.56 and 33.685 eV (Martin et al. 1999). In order to match the experimental series limits – obtained by extrapolating the $1s^2 2s 2p nl$ resonance positions to $n \rightarrow \infty$ – to these values a scaling factor 1.00564 was applied to the energy scale. This factor is within the experimental uncertainty.

Next to the $1s^2 2s 2p nl$ DR resonances, further resonances are attached to $2s^2 \rightarrow 2p^2$ double core excitations; they appear especially below the $1s^2 (2s 2p^3 P)$ series limit. The radiative decay of these *triply* excited resonance states to below the Mg ix ionization limit completes *trielelectronic* recombination (TR). The importance of TR for the photorecombination of

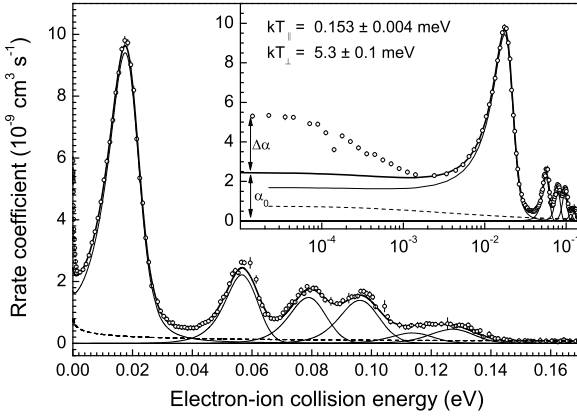


Fig. 2. High resolution Mg ix merged-beams recombination rate-coefficient in the energy range of the $1s^2(2s2p^3P)7l$ DR resonances close to zero electron-ion collision energy: Experiment (symbols) and RR and DR resonance fit (thick full line). Individual contributions to the fit are 6 DR resonances (thin full lines) and RR (thin dashed line). Data points below 3 meV were excluded from the fit. The electron beam temperatures resulting from the fit are indicated in the inset which shows the same data on a logarithmic energy scale. It emphasizes the excess recombination rate coefficient $\Delta\alpha$ at very low energies (see text). The maximum enhancement is $(\Delta\alpha + \alpha_0)/\alpha_0 \approx 2.3$. Further fit results are given in table 1.

berylliumlike ions was only recently discovered and discussed by Schnell et al. (2003). For berylliumlike Cl xiv they find that over the plasma temperature range 1–100 eV TR contributes up to 20–40% to the total recombination rate coefficient.

The disentanglement of TR and DR contributions to the measured recombination spectrum requires detailed atomic structure calculations and is beyond the scope of this paper. Therefore, only obvious TR contributions are marked in Figure 1. For a more detailed discussion of TR the reader is referred to the work of Schnell et al. (2003). For the present purpose of deriving the experimental Mg ix plasma rate coefficient the question of the origin of individual resonances is not relevant. In any theoretical calculation, however, TR has to be accounted for in order to arrive at an accurate Mg ix plasma rate coefficient.

3.2. Recombination at low energies

Figure 2 shows the experimental merged-beams Mg ix recombination rate coefficient from very low energies up to 0.17 eV. In this energy range, the recombination rate coefficient is dominated by $1s^2(2s2p^3P)7l$ DR resonances. For an accurate determination of the resonance parameters we fitted 6 DR resonance line profiles to the measured spectrum as well as a smooth contribution due to radiative recombination (RR). In the fit the corresponding cross sections $\sigma(E)$ were convoluted with the experimental electron energy distribution

$$f(E, \hat{E}, T_{\parallel}, T_{\perp}) = \frac{1}{k_B T_{\perp} \xi} \exp\left(-\frac{E - \hat{E}/\xi^2}{k_B T_{\perp}}\right) \quad (1)$$

$$\times \left[\operatorname{erf}\left(\frac{\sqrt{E} + \sqrt{\hat{E}}/\xi^2}{\sqrt{k_B T_{\parallel}}/\xi}\right) + \operatorname{erf}\left(\frac{\sqrt{E} - \sqrt{\hat{E}}/\xi^2}{\sqrt{k_B T_{\parallel}}/\xi}\right) \right].$$

It is characterized by the longitudinal and transversal — with respect to the electron beam direction — temperatures T_{\parallel} and T_{\perp} , respectively (Kilgus et al. 1992), and $\xi = (1 - T_{\parallel}/T_{\perp})^{1/2}$. Furthermore, k_B denotes Boltzmann’s constant and $\operatorname{erf}(x) = 2\pi^{-1/2} \int_0^x \exp(-t^2) dt$ is the error function.

The convolution of the recombination cross section with the above experimental electron energy distribution yields the experimental *merged-beams rate coefficient*

$$\alpha_{MB}(\hat{E}) = \int_0^{\infty} \sqrt{2E/m_e} \sigma(E) f(E, \hat{E}, T_{\parallel}, T_{\perp}) dE \quad (2)$$

where \hat{E} and m_e denote the experimental electron-ion collision energy and the electron rest mass, respectively. For each DR resonance the cross section was taken to be

$$\sigma^{(DR)}(E) = \frac{\bar{\sigma} E_{\text{res}}}{\pi E} \frac{\Gamma/2}{(E - E_{\text{res}})^2 + (\Gamma/2)^2}. \quad (3)$$

The DR line shape is assumed to be a Lorentzian multiplied by a factor E_{res}/E accounting for the $1/E$ dependence of the DR cross section at low energies (Schippers et al. 1998). For $E_{\text{res}} \gg \Gamma$ this factor can be neglected. In the limit $\Gamma \rightarrow 0$ the DR-resonance profile becomes a delta-function and the corresponding merged-beams rate coefficient can be expressed analytically as

$$\alpha_{MB}^{(DR)}(\hat{E}) = \bar{\sigma} \sqrt{2E_{\text{res}}/m_e} f(E_{\text{res}}, \hat{E}, T_{\parallel}, T_{\perp}) \quad (4)$$

with $f(E_{\text{res}}, \hat{E}, T_{\parallel}, T_{\perp})$ from Equation 1. For $\Gamma > 0$ the merged-beams rate coefficient $\alpha_{MB}^{(DR)}(\hat{E})$ was evaluated numerically.

For the radiative recombination (RR) cross section the semi-classical hydrogenic formula of Bethe & Salpeter (1957) was used in slightly modified form, i. e.,

$$\sigma^{(RR)}(E) = 2.105 \times 10^{-22} \text{ cm}^2 \sum_{n_{\min}}^{n_{\max}} k_n t_n \frac{(Z_{\text{eff}}^{\mathcal{R}})^2}{nE(Z_{\text{eff}}^{\mathcal{R}} + n^2E)} \quad (5)$$

and the convolution (Eq. 2) was performed numerically. In equation 5 the letter \mathcal{R} denotes the Rydberg constant. The effective charge was taken to be $Z_{\text{eff}} = 8$ and the summation over the principal quantum numbers n was carried out from $n_{\min} = 2$ to $n_{\max} = 44$. The latter value is determined by field ionization in the charge-state-analyzing dipole magnet (Schippers et al. 2001). The constants t_n account for partly filled shells. Here $t_2 = 6/8$ and $t_n = 1$ for $n > 2$ were used. The factors k_n correct for the deviation of the semi-classical cross sections from the more exact quantum mechanical results and were calculated following the prescription of Andersen & Bolko (1990). They are monotonically increasing for increasing n , starting from $k_2 = 0.877$ and approaching unity for higher n .

The resonance parameters that were obtained from the fit are listed in Table 1. The reduced χ^2 of the fit is 1.24. The electron beam temperatures resulting from the fit are $k_B T_{\parallel} = 0.153 \pm 0.004$ meV and $k_B T_{\perp} = 5.1 \pm 0.1$ meV. These values roughly correspond to what is expected from the electron cooler settings (Pastuszka et al. 1996). Data points

$E_{\text{res}} / [\text{meV}]$	$\Gamma / [\text{meV}]$	$\bar{\sigma} / [10^{-18} \text{ eV cm}^2]$
20.92(5)	4.6(1)	17.93(7)
60.2(1)	–	2.23(2)
82.5(1)	–	1.41(2)
99.9(2)	–	1.29(2)
117.6(9)	–	0.30(2)
131.0(4)	–	0.41(2)

Table 1. Results of fitting individual DR resonances to the measured recombination rate coefficient at low energies (Fig. 2). Each resonance is characterized by its resonance position E_{res} , width Γ and strength $\bar{\sigma}$. Numbers in brackets denote the statistical uncertainties obtained from the fit. If no value for the width is given a delta-function-like resonance was assumed.

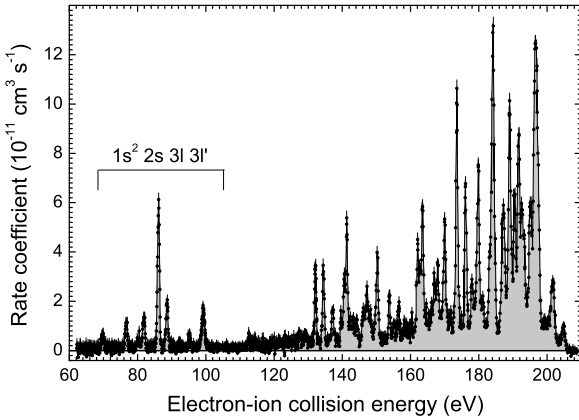


Fig. 3. Measured Mg ix merged-beams recombination rate-coefficient in the electron-ion collision energy region of DR $1s^2 2s 3l n'l$ resonances attached to $1s^2 2s^2 \rightarrow 1s^2 2s 3l$ ($\Delta N = 1$) core excitations.

below 3 meV were excluded from the fit. At lower energies the measured rate coefficient exceeds the fitted one by a factor of up to 2.3 (inset of Figure 2). This recombination rate enhancement at very low energies is an inherent feature of merged-beams experiments at electron coolers (Gwinner et al. 2000; Heerlein et al. 2002; Hörndl et al. 2003; Wolf & Gwinner 2003). In the present context, this recombination rate enhancement can be clearly distinguished from the normal photorecombination rate coefficient and is excluded from the experimentally derived plasma rate coefficient of Section 3.4.

3.3. $\Delta N = 1$ dielectronic recombination

Resonances attached to $1s^2 2s^2 \rightarrow 1s^2 2s 3l$ ($\Delta N = 1$) core excitations occur in the energy range 70-205 eV (Figure 3). The lowest resonances of this group are the $1s^2 2s 3l 3l'$ DR resonances extending to energies of up to about 100 eV. The higher- n manifolds of $1s^2 2s 3l n'l$ DR resonances mutually overlap. In contrast to $\Delta N = 0$ DR, the resonance strengths of the $\Delta N = 1$ DR resonances rapidly decrease with increasing n . Therefore,

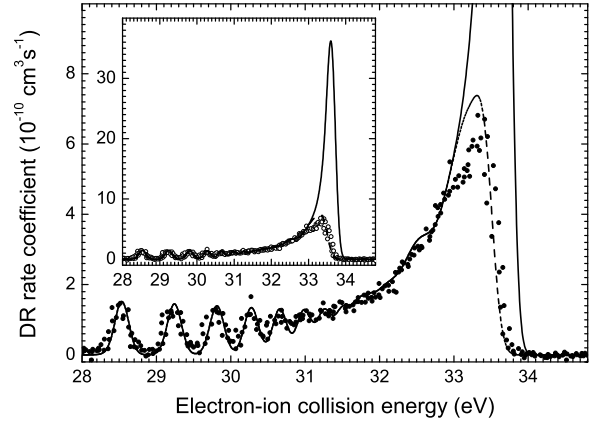


Fig. 4. Experimental merged-beams recombination rate coefficient in the region of high- n $1s^2 (2s 2p^1 P) nl$ DR resonances together with the result of an AUTOSTRUCTURE calculation scaled by a factor 0.7. The dashed line is the theoretical result with account for the experimental field ionization of high- n Rydberg states using the field-ionization model of Schippers et al. (2001). The full curve is the theoretical result including the full DR resonance strength up to $n = 1000$. The inset shows the same curves on a different scale for an overview.

the resonance strength does not pile up at the series limits. In Figure 3 two series limits can be discerned at 202.25 and 205.14 eV. In order to match these values from the NIST atomic spectra data base (Martin et al. 1999) for the $1s^2 2s 3d^1 D nl$ and the $1s^2 2s 3d^3 D nl$ series, respectively, the experimental energy scale was multiplied by a factor 1.0091. This rescaling is within the experimental uncertainty.

3.4. Plasma recombination rate coefficient

Formally, the recombination rate-coefficient in a plasma is obtained by using an isotropic Maxwellian distribution function in equation 2, i. e.,

$$\alpha_{\text{plasma}}(k_B T) = \frac{4}{\sqrt{2\pi m_e} (k_B T)^{3/2}} \int_0^\infty \sigma(E) E \exp\left(-\frac{E}{k_B T}\right) dE. \quad (6)$$

For plasma temperatures $k_B T \gg k_B T_\perp$ a factor $\sigma(E) \sqrt{2E/m_e}$ in the integral may be replaced by the experimental merged-beams recombination rate coefficient. This approach can safely be used for all recombination resonances with $E_{\text{res}} \gg k_B T_\perp$. Here it was applied to all recombination resonances above 0.2 eV that are shown in Figures 1 and 3. In order to exclude any effect of the finite experimental energy spread on the experimentally derived plasma rate coefficient, Equation 6 was used with the resonance cross section from Equation 3 for the resonances at lower energies. The contribution of the recombination resonances below 0.2 eV (Figure 2) to the plasma recombination rate-coefficient was evaluated by using the fitted resonance parameters from Table 1.

For the derivation of the experimental Mg ix recombination rate coefficient one has to be aware of the fact that loosely

i	$c_i / [\text{cm}^3 \text{s}^{-1} \text{K}^{3/2}]$	$E_i / [\text{eV}]$
1	3.5960×10^{-2}	2.0071×10^6
2	2.0109×10^{-2}	3.7011×10^5
3	2.6244×10^{-3}	1.2038×10^5
4	3.6203×10^{-4}	4.5163×10^4
5	4.1121×10^{-5}	9.2881×10^2
6	2.6915×10^{-5}	2.2683×10^2
7	6.7347×10^{-7}	3.7786×10^1

Table 2. Parameters for the fit of equation 7 to the experimentally derived Mg ix DR+TR rate coefficient in a plasma. In the temperature ranges 25–350 K and $350\text{--}9 \times 10^8$ K the fit deviates less than 2% and 1%, respectively, from the experimentally derived result. The systematic uncertainty of the experimentally derived absolute recombination rate coefficient is $\pm 15\%$ (Lampert et al. 1996).

bound high- n Rydberg states are easily field ionized in our experimental setup. This effect was modelled in considerable detail by Schippers et al. (2001). Generally, it is more significant for lower charged ions. As shown in Figure 4 a theoretical calculation of the Mg ix DR rate coefficient using the AUTOSTRUCTURE code of Badnell (1986) can only be reconciled with the experimental data if field-ionization is taken into account.

In the present case the effect of field-ionization on the measured DR spectrum can be approximately described as a cutoff of high- n Rydberg resonances with $n \gtrsim 44$. In order to account for the unmeasured DR resonance strength the DR spectrum for $n < 44$ is extrapolated to higher n by scaling the result of the AUTOSTRUCTURE calculation to the experimental spectrum in the energy range 28.0–32.9 eV (scaling factor 0.7, Figure 4) and by replacing the measured merged-beams rate coefficient by the scaled calculated value in the energy range 32.9–34.1 eV.

In principle, such a correction also has to be made for all other series of Rydberg resonances. For $\Delta N = 0$ DR such other series are relatively weak (Figure 1) and their cutoff by field-ionization does not lead to a significant error when considering the overall $\pm 15\%$ experimental uncertainty of the absolute rate coefficient scale (Lampert et al. 1996). Regarding $\Delta N = 1$ DR, the resonance strength, as already mentioned, decreases strongly with increasing n , leading again to a negligible effect of the experimental field-ionization on the plasma rate coefficient.

Our experimentally derived Mg ix DR+TR recombination rate coefficient in a plasma — including the extrapolation of the $1s^2(2s2p^1P)nl$ resonance strength to $n = 1000$ (cf. Figure 4) — is shown in Figure 5 as a thick full line. For the convenient use of our result in plasma modelling codes the following functional dependence — customarily used for DR rate coefficients — was fitted to our experimentally derived curve:

$$\alpha_{\text{fit}}^{(\text{DR})} = \frac{1}{T^{3/2}} \sum_i c_i \exp\left(-\frac{E_i}{k_B T}\right). \quad (7)$$

During the fitting procedure the coefficients c_i and E_i were varied. The fit results are listed in Table 2.

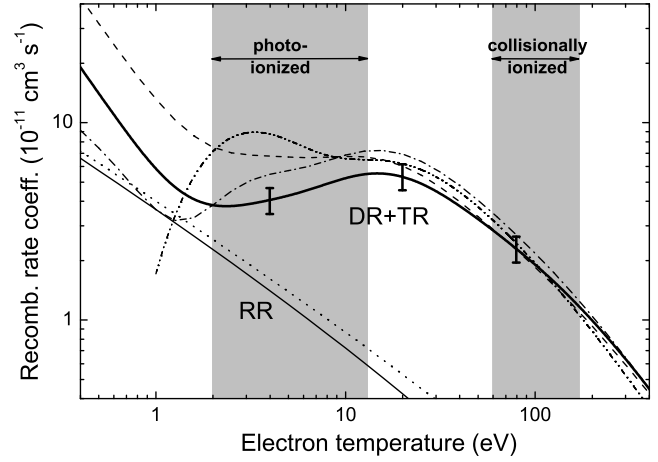


Fig. 5. Comparison of the present experimentally derived Mg ix DR rate coefficient (thick full line) with the recommendation of Mazzotta et al. (1998, dash-dot-dotted line) and the theoretical results of Gu (2003a, dashed line) and Colgan et al. (2003, dash-dotted line). The error bars denote the $\pm 15\%$ experimental uncertainty of the absolute rate coefficient. The thin full line is the RR rate coefficient calculated (eq. 6) with the RR cross section from equation 5 with $n_{\text{max}} = 1000$ and the remaining RR parameters from section 3.2. The dotted line is the theoretical RR rate coefficient of Gu (2003b). The temperature ranges (see section 1) where Mg ix exists in photoionized and in collisionally ionized plasmas, respectively, are highlighted.

In the fit to the low-energy experimental merged-beams recombination rate coefficient (Figure 2) RR was also included (with T_{\parallel} and T_{\perp} as the only free fit parameters and all other parameters kept fixed). The same RR cross section was used to draw the RR contribution in Figure 1. This shows that Equation 5 for the RR cross section is consistent with our experimental data. Therefore, Equation 5, in conjunction with Equation 6, can also be used to derive the experimental Mg ix RR rate coefficient in a plasma.

To this end, the RR cross section parameters were taken from section 3.2. In order to make up for field-ionization effects the plasma RR rate coefficient in Figure 5 (thin full line) was calculated with $n_{\text{max}} = 1000$ instead of $n_{\text{max}} = 44$ as in Figure 2. For convenient further use our Mg ix RR rate coefficient in a plasma was fitted by a formula introduced by Verner & Ferland (1996):

$$\alpha_{\text{fit}}^{(\text{RR})} = A \left[\sqrt{\frac{T}{T_0}} \left(1 + \sqrt{\frac{T}{T_0}} \right)^{1-b} \left(1 + \sqrt{\frac{T}{T_1}} \right)^{1+b} \right]^{-1}. \quad (8)$$

The parameter values that were obtained from the fit are $A = 5.7414 \times 10^{-10} \text{ cm}^3 \text{ s}^{-1}$, $b = 0.67692$, $T_0 = 206.15 \text{ K}$, and $T_1 = 7.6200 \times 10^6 \text{ K}$. Over the temperature ranges $1\text{--}2.9 \times 10^6 \text{ K}$ and $2.9 \times 10^6\text{--}10^8 \text{ K}$ the fit is accurate to more than 2% and 3%, respectively.

In Figure 5 the present experimentally derived RR rate coefficient is compared with the recent theoretical result of Gu (2003b, dotted line). The difference is less than 17% over the temperature range where Mg ix exists in a photoionized plasma.

The total (unified) Mg ix recombination rate coefficient is readily obtained as the sum of our DR+TR and RR rate coefficients. It should be noted that this result does not depend on the existence of possible quantum mechanical interferences between RR and DR, since interference has already been neglected during the decomposition of the measured spectrum into DR and RR (Figure 2). In principle, interference between RR and DR can lead to asymmetric recombination resonance line shapes (see e. g. Schippers et al. 2002). No evidence for such effects is found in our experimental Mg ix recombination spectra. The systematic uncertainty of the experimentally derived total Mg ix recombination rate coefficient is $\pm 15\%$ (Lampert et al. 1996).

4. Discussion and Conclusions

In Figure 5 the present experimentally derived DR+TR rate coefficient is compared with the recommendation of Mazzotta et al. (1998) and with the recent calculations of Gu (2003a) and Colgan et al. (2003). The recommended Mg ix DR rate coefficient of Mazzotta et al. (1998) deviates by up to 130% from the experimental result in the temperature range 2–13 eV where Mg ix exists in photoionized plasmas. This rather large discrepancy questions the usefulness of the recommended Mg ix DR rate coefficient for the modeling of photoionized plasmas. In the temperature range 60–170 eV (collisionally ionized zone) the recommended Mg ix DR rate coefficient of Mazzotta et al. (1998) agrees within 11%, i. e., within the 15% experimental uncertainty, with the experimentally derived one.

In this temperature range the theoretical rate coefficient of Gu (2003a) shows very good agreement with the experimentally derived rate coefficient. The difference between the two curves in this range is less than 7%. At lower temperatures, however, the discrepancy is up to 99% at 2 eV. At these low temperatures where Mg ix exists in photoionized plasmas, the theoretical result of Colgan et al. (2003) agrees better with the experimental rate coefficient. The deviation is less than 35% for $k_B T > 2$ eV, less than 30% for $k_B T > 15$ eV, and less than 15% for $k_B T > 100$ eV. At the temperature 2.8 eV where the fractional abundance of Mg ix is expected to peak in a photoionized plasma (Kallman & Bautista 2001) the results of Gu (2003a) and Colgan et al. (2003) deviate from the experimental rate coefficient by 82% and 25%, respectively.

The rather large low-temperature deviation of the theoretical rate coefficient of Gu (2003a) from the experimentally derived curve is most probably due to an inaccurate calculation of the DR resonance energies below 0.15 eV (Figure 2). At these very low energies the DR rate coefficient is very sensitive to slight variations of resonance positions. This is highlighted in Figure 6 that displays the effect of hypothetical shifts of the low-energy resonance positions by ± 50 meV and ± 100 meV with respect to the tabulated values (Table 1) on the Mg ix DR rate coefficient. Obviously, a ± 100 meV uncertainty of the low-energy $1s^2(2s2p^3P)7l$ resonance positions translates into an uncertainty of a factor 2.7 of the plasma rate coefficient in the temperature range where the fractional abundance of Mg ix peaks in a photoionized gas.

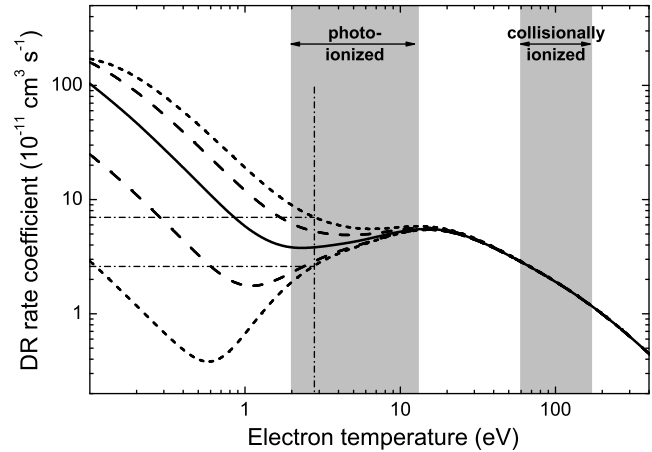


Fig. 6. Impact of a shift of the low energy $1s^2(2s2p^3P)7l$ resonances displayed in Figure 2 on the Mg ix DR plasma rate-coefficient. The full curve is the experimental result, the long-dashed curves correspond to resonance shifts of $\Delta E_{\text{res}} = \pm 50$ meV, and the short-dashed curves to a shift of $\Delta E_{\text{res}} = \pm 100$ meV. Thereby, the lower curves correspond to resonance shifts to lower energies. The vertical dash-dotted line marks the temperature 2.8 eV where the fractional abundance of Mg ix peaks in a photoionized gas (Kallman & Bautista 2001). The horizontal dash-dotted lines indicate the factor 2.7 uncertainty of the plasma rate coefficient at this temperature that would be introduced by a ± 100 meV uncertainty of the low energy resonance positions.

These findings demonstrate that an accurate calculation of DR rates for ions that exhibit DR resonances close to zero energy is challenging. In case of more complex ions this task is certainly beyond the capabilities of present-day atomic structure codes as is exemplified by a recent combined theoretical and experimental DR study of argon-like Sc^{3+} (Schippers et al. 2002). Recombination experiments at heavy-ion storage rings are certainly required for guiding the future development of the theoretical methods, especially in the case of low temperature DR rate coefficients for complex ions.

Acknowledgements. We thank D. W. Savin for helpful discussions and the MPI-K accelerator crew, in particular R. Reppow and M. Grieser, for their excellent support. This work was partly funded by Deutsche Forschungsgemeinschaft under contract Mu 1068/8.

References

- Andersen, L. H. & Bolko, J. 1990, Phys. Rev. A, 42, 1184
- Badnell, N. R. 1986, J. Phys. B, 19, 3827, <http://amdpp.phys.strath.ac.uk/autos/>
- Badnell, N. R., Pindzola, M. S., Andersen, L. H., Bolko, J., & Schmidt, H. T. 1991, J. Phys. B, 24, 4441
- Bethe, H. A. & Salpeter, E. E. 1957, Quantum Mechanics of One- and Two-Electron Atoms (Berlin: Springer)
- Böhm, S., Müller, A., Schippers, S., et al. 2003, Astron. Astrophys., 405, 1157
- Colgan, J., Pindzola, M. S., Whiteford, A. D., & Badnell, N. R. 2003, Astron. Astrophys., 412, 597

- Fogle, M., Badnell, N. R., Eklöw, N., Mohamed, T., & Schuch, R. 2003, *Astron. Astrophys.*, 409, 781
- Gu, M. F. 2003a, *Astrophys. J.*, 590, 1131
- Gu, M. F. 2003b, *Astrophys. J.*, 589, 1085
- Gwinner, G., Hoffknecht, A., Bartsch, T., et al. 2000, *Phys. Rev. Lett.*, 84, 4822
- Heerlein, C., Zwicknagel, G., & Toepffer, C. 2002, *Phys. Rev. Lett.*, 89, 083202
- Hörndl, M., Yoshida, S., Tökési, K., & Burgdörfer, J. 2003, *Hyperfine Interact.*, 146/147, 13
- Kallman, T. & Bautista, M. 2001, *Astrophys. J. Suppl. Ser.*, 133, 221
- Kilgus, G., Habs, D., Schwalm, D., et al. 1992, *Phys. Rev. A*, 46, 5730
- Lampert, A., Wolf, A., Habs, D., et al. 1996, *Phys. Rev. A*, 53, 1413
- Martin, W. C., Sugar, J., Musgrove, A., et al. 1999, *NIST Atomic Spectra Data Base*, 2nd edn., National Institute of Standards and Technology, Gaithersburg, Maryland 20899-3460, USA, http://physics.nist.gov/cgi-bin/AtData/main_asd
- Mazzotta, P., Mazzitelli, G., Colafrancesco, S., & Vittorio, N. 1998, *Astron. Astrophys.*, 133, 403
- Müller, A. & Wolf, A. 1997, in *Accelerator-based atomic physics techniques and applications*, ed. J. C. Austin & S. M. Shafroth (Woodbury: AIP Press), 147
- Pastuszka, S., Schramm, U., Grieser, M., et al. 1996, *Nucl. Instrum. Methods A*, 369, 11
- Phaneuf, R. A., Havener, C. C., Dunn, G. H., & Müller, A. 1999, *Rep. Prog. Phys.*, 62, 1143
- Poth, H. 1990, *Phys. Rep.*, 196, 135
- Savin, D. W., Bartsch, T., Chen, M. H., et al. 1997, *Astrophys. J. Lett.*, 489, L115
- Savin, D. W., Behar, E., Kahn, S. M., et al. 2002a, *Astrophys. J. Suppl. Ser.*, 138, 337
- Savin, D. W., Kahn, S. M., Gwinner, G., et al. 2003, *Astrophys. J. Suppl. Ser.*, 147, 421
- Savin, D. W., Kahn, S. M., Linkemann, J., et al. 1999, *Astrophys. J. Suppl. Ser.*, 123, 687
- Savin, D. W., Kahn, S. M., Linkemann, J., et al. 2002b, *Astrophys. J.*, 576, 1098
- Schippers, S., Bartsch, T., Brandau, C., et al. 1998, *J. Phys. B*, 31, 4873
- Schippers, S., Bartsch, T., Brandau, C., et al. 2000, *Phys. Rev. A*, 62, 022708
- Schippers, S., Kieslich, S., Müller, A., et al. 2002, *Phys. Rev. A*, 65, 042723
- Schippers, S., Müller, A., Gwinner, G., et al. 2001, *Astrophys. J.*, 555, 1027
- Schnell, M., Gwinner, G., Badnell, N. R., et al. 2003, *Phys. Rev. Lett.*, 91, 043001
- Verner, D. A. & Ferland, G. J. 1996, *Astrophys. J. Suppl. Ser.*, 103, 467
- Wolf, A. & Gwinner, G. 2003, *Hyperfine Interact.*, 146/147, 5